IL NUOVO CIMENTO **41 C** (2018) 108
DOI 10.1393/ncc/i2018-18108-6

COMMUNICATIONS: SIF Congress 2017

Charge identification of galactic cosmic rays with the DAMPE mission

M. DI SANTO(1)(2)(*) on behalf of the DAMPE COLLABORATION

(1) *Dipartimento di Matematica e Fisica "Ennio De Giorgi", Università del Salento - Via per Arnesano, I-73100 Lecce, Italy*
(2) *INFN, Sezione di Lecce - Via per Arnesano, I-73100 Lecce, Italy*

received 30 January 2018

Summary. — DAMPE (DArk Matter Particle Explorer) is a space mission project promoted by the Chinese Academy of Sciences (CAS), in collaboration with Universities and Institutes from China, Italy and Switzerland. The detector was successfully launched on orbit on December 17th, 2015 from the Jiuquan Satellite Launch Center, and it is right now in a stable data acquisition. The main goals of the mission are: indirect search of Dark Matter, looking for signatures in the electron and photon spectra with energies up to 10 TeV; analysis of the flux and composition of primary cosmic rays with energies up to hundreds TeV; high energy gamma ray astronomy.

1. – Introduction

The direct detection of galactic Cosmic Rays, their elemental analysis, the energy spectrum and incidence direction reconstruction are the main goals of a research devoted to better understand where these particles come from and by which mechanisms they are accelerated all around the Galaxy. Several detectors have been installed on the International Space Station ISS (AMS-02, ref. [1]) or on satellites (FERMI, ref. [2]; PAMELA, ref. [3]), each one with specific features, in order to detect events of galactic Cosmic Rays and to reconstruct their flux as a function of the measured kinetic energy. DAMPE (DArk Matter Particle Explorer) is a satellite-borne particle detector, one of the five projects of the Strategic Pioneer Program on Space Science, the space exploration programme of the Chinese Academy of Sciences (CAS). Thanks to its features, DAMPE is able to record events of electrons, γ-rays, protons, helium and heavier nuclei with a very good resolution in a large energy range. It is smoothly collecting data in a stable

(*) E-mail: margherita.disanto@le.infn.it

Sun-synchronous orbit lasting 95 minutes at an altitude of about 500 km since December 17th, 2015, day of its launch from the Gobi Desert.

The primary goal of this mission is to give an important contribution to the research of Dark Matter by probing its nature. Recently, DAMPE obtained an important result in this field, see ref. [4], showing the direct measurement of cosmic electrons and positrons in the energy range of 25 GeV−4.6 TeV, with unprecedentedly high energy resolution and low background and, in particular, showing a spectral break at $\sim$ 0.9 TeV. This measure can take, moreover, to a better understanding of possible sources like pulsars which can be close to our Solar system.

In addition to recording cosmic ray nuclei events finalized to fluxes measurements and studies of the accelaration and propagation mechanisms, the satellite works also as γ-ray observatory in Space, searching for new photon sources in the high energy range, like Gamma Ray Bursts (GRBs), Active Galactic Nuclei (AGN) and other transient objects. In this paper, the discussion will be focused on the energy loss measurement and the subsequent charge reconstruction of galactic Cosmic Rays by using mainly the first sub-detector of DAMPE, the Plastic Scintillation Detector (PSD). It will start from a short description of the detector and its characteristics, then the methods for event selection and charge reconstruction of the incoming particles will be discussed. Finally, some preliminary results about the *All-Z* charge spectrum and the proton and helium fluxes will be shown.

2. – The DAMPE detector

DAMPE is mainly composed by 4 sub-detectors, as shown in fig. 1. They are, from the top to the bottom, the following:

1) *Plastic Scintillation array Detector* (*PSD*), that gives a measurement of the absolute value of the charge of incident high energy particles (with $Z \leq 28$) and it is also used as anti-coincidence system for γ-rays;

2) *Silicon-Tungsten tracKer-converter* (*STK*) used for the trajectory reconstruction of incoming particles and, moreover, for a further measurement of charge;

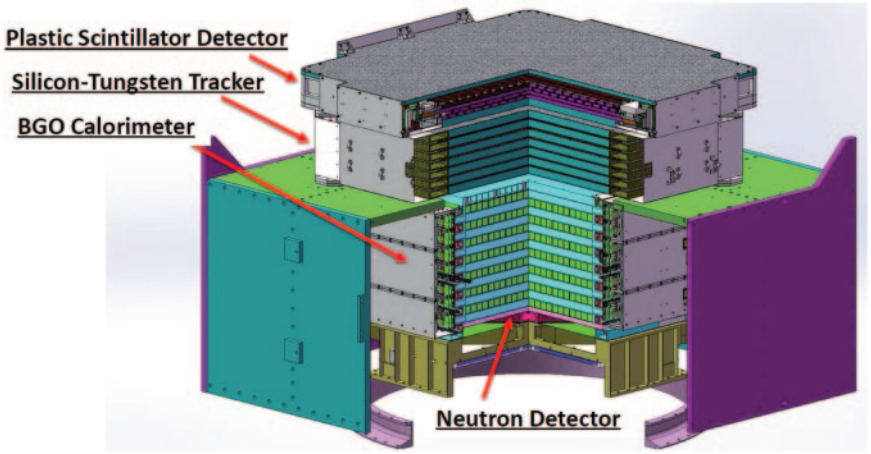

Fig. 1. – 3D view of the DAMPE detector.

3) *BGO calorimeter* (*BGO*) which provides the energy measurement, the electron and hadron identification and an additional contribution to the track reconstruction;

4) *NeUtron Detector* (*NUD*) that gives further information for electron/hadron discrimination.

2˙1. *Plastic Scintillation array Detector (PSD).* – The PSD is the first detector on the top of the satellite, with an active area of 82.5 cm × 82.5 cm. It is mainly composed by two planes with a double layer configuration (done to reduce the back-splash effect) and a total number of 82 bars of plastic scintillator EJ-200, produced by Eljen Technology Corporation. The choice of EJ-200 is due to the good features that it provides, like relatively high light output, time performance (0.9 ns rise time and 2.1 ns decay time), a large bulk light attenuation length (380 cm) and the scintillation emission centered on a wavelength of 425 nm. Each bar has a dimension of 884 mm × 28 mm × 10 mm, with a *double-end* readout system composed by two low-noise Photo Multiplier Tubes (PMTs R4443 manufactured by Hamamatsu Photonics) coupled at the ends of the single bar with optical pads. The detector modules (bar&PMTs) are parallel to each other in one layer and orthogonal to the scintillators located in the other layer. In other words, the bars of the upper layer are parallel to the X axis, while the bars at the bottom are parallel to the Y axis, where the coordinate system, shown in fig. 2, has been chosen in such a way that the Z axis is oriented to the zenith, orthogonal to all the detector's planes and the Y axis points to the Sun. Since, according to the Bethe-Bloch formula, the energy deposition of a particle with atomic number Z is $\propto Z^2$, to detect cosmic-ray nuclei from protons to nickel ($Z = 28$) with the PSD, a wide dynamic range is necessary for the output signals as well as for the read-out unit of PSD bars.

The dynamic range can be estimated by using as unit the Minimum Ionizing Particle (MIP), which is defined as the mean light yield by a singly charged particle with a normal incidence direction hitting the center of a single PSD bar. The energy deposition of a MIP for the PSD bar is $\sim$ 2 MeV. The request for the dynamic range is to be from 0.1 MIPs to 1400 MIPs for each PMTs with a good resolution. This has been possibile by using for each PMT the signal from a low gain dynode (the 5th), which covers a range between 0.1 MIPs to 40 MIPs, coupled with a high gain dynode (the 8th) that covers a range between 4 MIPs to 1600 MIPs. The overlap between the signals of two dynodes can be used for calibration. The charge resolution, obtained by using a Gaussian distribution, is $\leq 25\%$ for $Z = 1$.

2˙2. *Silicon-Tungsten tracKer-converter (STK).* – The second sub-detector starting from the top of the satellite is the STK, whose general scheme is shown in fig. 3. It is composed by six planes of trackers, each plane made of two 76 cm × 76 cm *single-sided* silicon layers, one for the X direction and the other for the Y direction. These layers have a thickness of 320 μm and each one is segmented in 16 modules, each with 768 AC - coupled p-strips implanted in the n-doped bulk with a strip pitch of 121 μm. The silicon strips have a read-out pitch of 242 μm with each module equipped with 6 VA140 ASIC (made by Gamma Medica-Ideas AS), a 64 channels low-power analog amplifier with high dynamic range, based on read-out chips for silicon trackers designed for the AMS experiment. Thanks to the analog read-out system, the spatial resolution is $< 80\,\mu$m within 60 ° of incidence. There are also three thin tungsten layers of thickness 1.0 mm placed between the 2nd, the 3rd and the 4th planes to increase the probability of high energy photons conversion in e^+/e^- pairs. For converted photons the angular resolution is ~ 0.2 °s at 10 GeV.

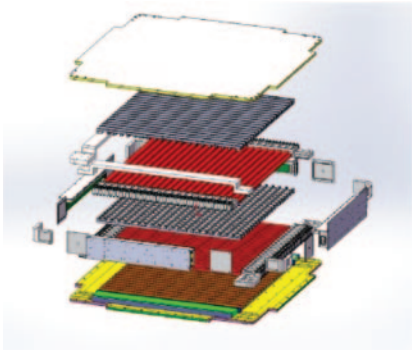

Fig. 2. – Main scheme of the PSD and representation of the coordinate system used for DAMPE.

2˙3. *BGO calorimeter (BGO).* – The DAMPE calorimeter consists of 14 layers with a total area of 60 cm × 60 cm and a depth of ∼ 31 radiation lengths, which means ∼ 1.6 interaction lengths (∼ 40 cm), and a weight of 830 kg. Each layer, as shown in fig. 4, constists of 22 crystal bars of $Bi_3Ge_4O_{12}$ (BGO) with dimensions 2.5 cm×2.5 cm×60.0 cm. The choice of the *Bismuth germanium oxide* is due to some very good features of this crystal, like the high Z which means a good photoelectric γ-rays conversion efficiency, the high γ-rays detection efficiency (3 times higher than that of NaI for 1 MeV photons), the high density ($\sim 7.1\,\mathrm{g/cm^3}$) and a short attenuation length. The crystal bars of adjacent layers are placed in such a way that their directions are orthogonal to each other, so it is possible to measure not only the deposited energy but also the longitudinal and transverse shower profiles in order to distinguish between electromagnetic and hadron showers. Each crystal bar has a *double-end* asimmetric read-out system with two PMTs (R5610A-01 made by Hamamatsu) coupled to them, one with an high gain output (called Side 0) and the other one with a low gain output (Side 1). The signal from Side 0 is about five times larger than that from Side 1, due to the different optical filters applied to the two sides and their specific attenuation factors on the scintillation light produced inside the calorimeter. In order to have a wide dynamic range of the energy deposition, a multi-dynode read-out circuit for the PMTs is used. In particular, dynodes 2, 5 and 8 are used, which correspond respectively to the lower, the medium and the higher gain signals from each PMT. The energy response of one BGO bar is from 10 MeV to 2 TeV.

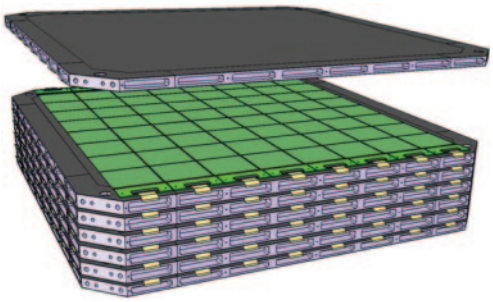

Fig. 3. – Schematic view of the DAMPE STK with its 12 layers of silicon micro-strip detectors mounted on 7 support trays and 3 tungsten plates integrated inside.

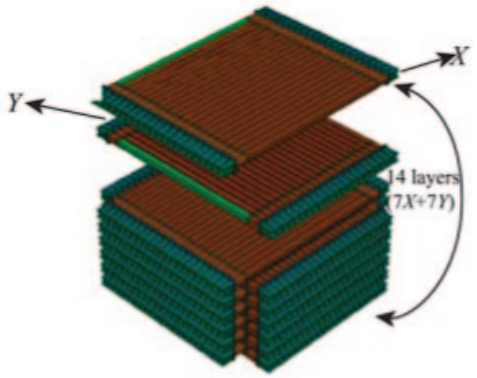

Fig. 4. – Arrangement of the BGO bars in 14 layers inside the DAMPE calorimeter. They are alternated layer by layer in an orthogonal way to detect the profile of showers generated inside the calorimeter.

The energy range in which the BGO can operate is 5 GeV–10 TeV for electrons and γ-rays with an energy resolution of $\sim 1.5\%$ at 800 GeV, while for protons and heavier nuclei the accessible energy range is 50 GeV–100 TeV with a resolution $< 40\%$ at 800 GeV.

2˙4. *NeUtron Detector (NUD).* – The last sub-detector of the satellite is the Neutron Detector, whose task is to improve the electron/hadron separating capability by detecting neutrons produced in showers generated inside the BGO calorimeter for primaries with energies higher than 100 GeV. The hadronic showers are characterized by a higher number of neutrons with respect to the electromagnetic-induced ones (in some cases, there is a difference of almost one order of magnitude between the relative abundances of neutrons). Neutrons thermalize after few microseconds and they can be detected by the NUD observing the result of the neutron capture process $^{10}\mathrm{B}+n \rightarrow {}^{7}\mathrm{Li}+\alpha+\gamma$, a nuclear reaction which can be observed with a transition probability inversely proportional to the speed of neutrons and a delay time lower than 2.5 μs from the beginning of the shower.

The NUD, see fig. 5, is mainly composed by a single layer with 4 large area boron-doped plastic scintillators with dimensions 30 cm $\times$ 30 cm $\times$ 1 cm, each one enveloped with a layer of aluminum film for photon reflection, and readout by a 10 dynode PMT located in the external corner coupled to a wavelength shifter which reduces the attenuation in optical transmission and increases photon collection efficiency.

More details about the structure of DAMPE, the specific features of the four sub-detectors, the performances and operations are well explained in ref. [5].

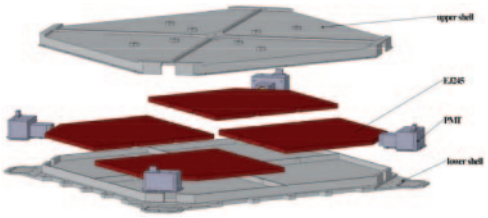

Fig. 5. – Schematic view of the DAMPE NUD composed by four boron-loaded plastics, each one equipped with a PMT and the related electronics.

3. – Charge reconstruction of galactic Cosmic Rays

3˙1. *Event selection criteria.* – In this paper, the methods used for the charge reconstruction of galactic Cosmic Rays and some preliminary results will be presented, all obtained by using the measure of the energy deposited inside the PSD, the tracks detected by the STK and the estimation of the total energy with the BGO calorimeter. DAMPE allows to investigate the events of galactic nuclei in the energy range 20 GeV–100 TeV with a good geometrical acceptance of $\sim 0.3\,\mathrm{m}^2\mathrm{sr}$. The DAMPE detector is in a stable data-taking with a trigger rate of $\sim 50\,\mathrm{Hz}$. The dead time of the satellite is mainly due to three contributions: the lapse in which the detector crosses the South Atlantic Anomaly (SAA) region ($\sim 4.5\%$ of the operation time), the on orbit calibration data-taking ($\sim 1.5\%$ of the operation time) and the instrumental dead time.

Once all the events recorded by DAMPE in the SAA are excluded, the remaining events are then subjected to a careful selection which consists in a series of cuts:

- cut 0 : all the events with a total energy deposited inside the BGO calorimeter higher than 20 GeV are selected;
- cut 1 : High Energy Trigger cut done in order to reject the minimum ionizing particles (MIPs), which means the selection of events with an energy release higher than $\sim 10\,\mathrm{MIP}$ ($1\,\mathrm{MIP} = 23\,\mathrm{MeV}$) inside the first 4 layers of the BGO;
- cut 2 : at least one reconstructed track in the STK;
- cut 3 : compatibility between the STK track direction and the position of the hit on the PSD bars (see fig. 6);
- cut 4 : match between the direction of the STK track and the direction of the BGO shower (see fig. 6) and, in case of more than one track, the closest to the BGO shower direction will be selected;
- cut 5 : charge identification;
- cut 6 : discrimination between electromagnetic and hadronic induced event.

These selection criteria of events have led to a good agreement between our analysis of flight-data and the Monte Carlo simulations in the case of protons and helium nuclei.

3˙2. *Charge measurement with the PSD.* – The method used for charge reconstruction of the incoming Cosmic Rays crossing the PSD starts from the calibration of the detector. The first step is to subtract the pedestals from the signals and then to perform the dynode calibration. As said in sect. **2**˙1, every PMTs coupled to one end of a PSD bar has a double-dynode readout and, in particular, both the signals from the low gain dy5 and the high gain dy8 are considered, in order to ensure a large dynamic range. What we do is to take as ADC value for each PMT the following:

$$ADC = \begin{cases} ADC_8 & \text{if } ADC_8 \leq 1100; \\ kADC_5 + c & \text{if } ADC_8 > 1100, \end{cases} \tag{1}$$

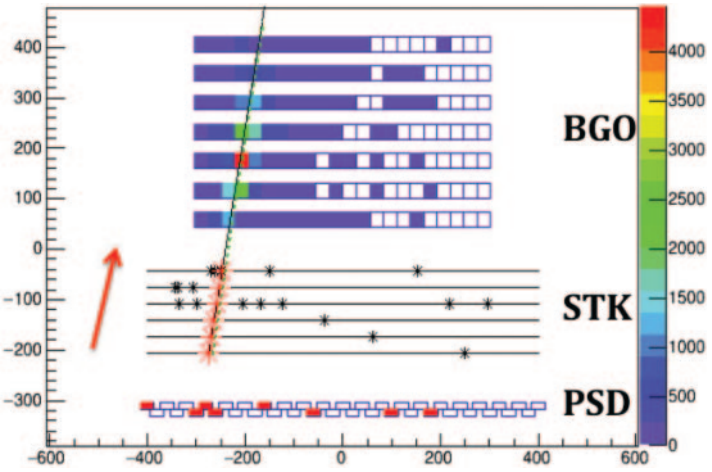

Fig. 6. – XZ view (reversed from the bottom to the top of the detector) of a match between the direction of a shower generated inside the BGO, a reconstructed STK track and PSD bars signals.

where k is the ratio between the two dynode signals (*slope parameter*) and C is the intersection parameter. From this the energy deposition recorded from a single side of a PSD bar can be evaluated using the following formula:

$$E = \frac{ADC}{A(x)} \times 2\,\mathrm{MeV}, \tag{2}$$

where $A(x)$ is a function which describes the attenuation of the scintillation light inside the bar during its propagation as a function of the hit position x (taken from the reconstructed track).

From the reconstructed single-side energy deposition, the (single-side) charge of the particle can be calculated as

$$Q^{Rec} = \sqrt{\frac{E}{E_{MIP}}}, \tag{3}$$

by considering that the energy deposition of a MIP per cm is equal to 2 MeV. The final step is to correct the expression (3) from the quenching effect, which reduces the scintillation efficiency of the organic scintillator. This correction is performed by using a parametrized Birk's law function (see ref. [6]),

$$Q^{corr} = f(Q^{Rec}). \tag{4}$$

For more details about these operations, see ref. [7].

4. – Preliminary results

By using the method of charge reconstruction explained in sect. **3**˙2, the preliminary result on the Cosmic Ray charge spectrum has been obtained.

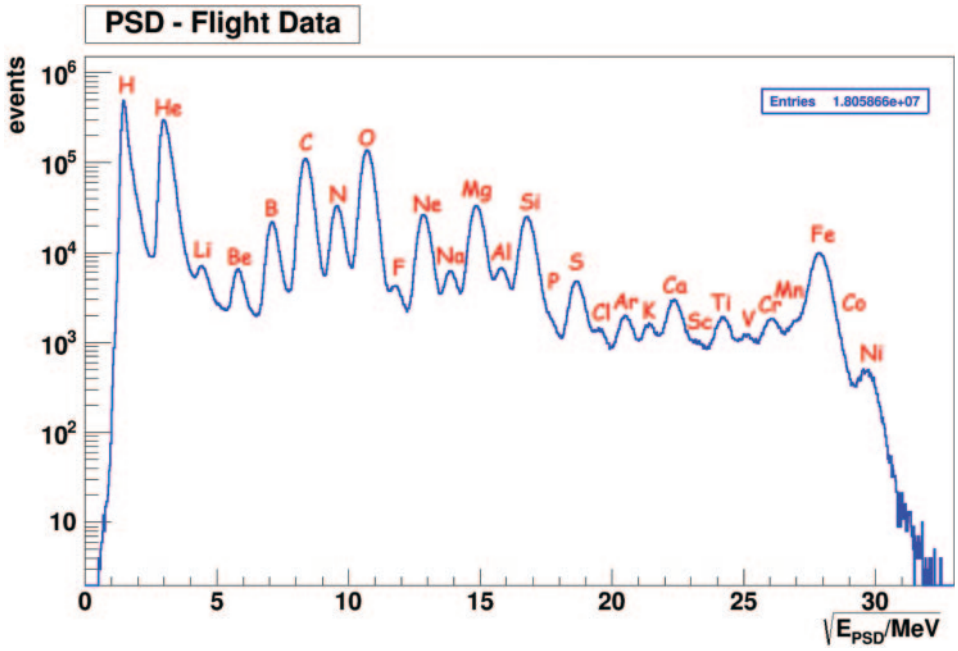

Fig. 7. – The *All-Z* charge spectrum reconstructed with the 17 months of data by using the square root of the energy deposition inside the PSD.

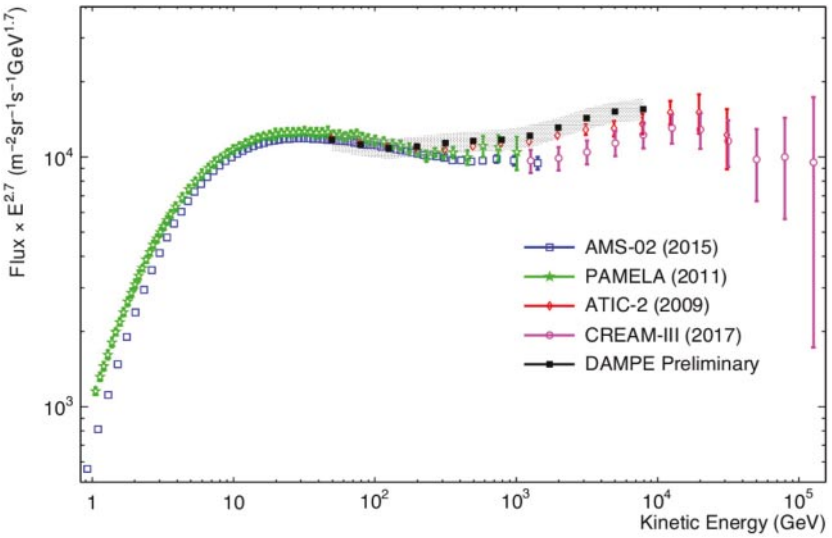

Fig. 8. – Preliminary Cosmic Ray proton flux measured by DAMPE compared with other experiments (AMS-02 [8], PAMELA [9], ATIC-2 [10], CREAM-III [11], DAMPE [12]). The statistical errors are plotted with bars while the systematics are represented by the grey band.

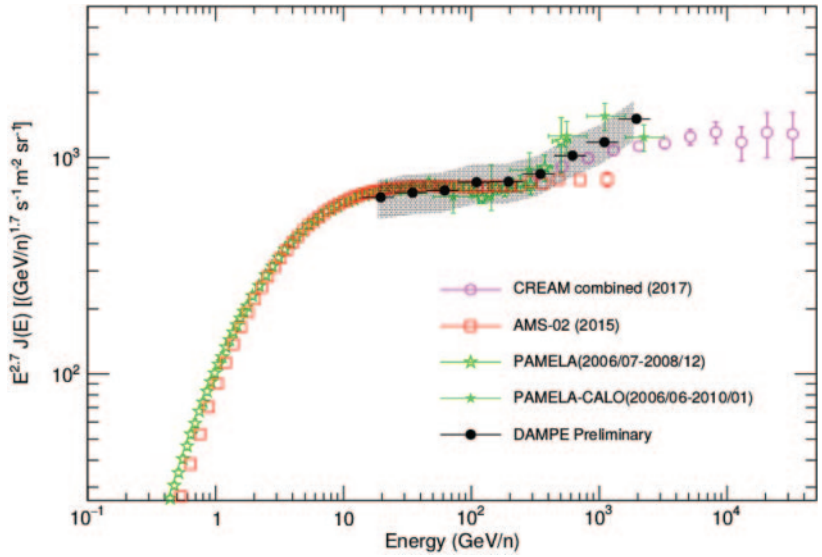

Fig. 9. – Preliminary Cosmic Ray helium flux measured by DAMPE in a good agreement with the previous results of other experiments (AMS-02 [13], PAMELA [9], CREAM [11], DAMPE [14]). The statistical errors are plotted with bars while the systematics are represented by the grey band.

In fig. 7 there is the *All-Z* charge spectrum obtained with 17 months of data acquisition. It shows the number of events as a function of the square root of the arithmetic mean calculated for the energies in the two views XZ and YZ of the PSD. This value has been then transformed in a dimensionless number by dividing it for 1 MeV, so, according to the Bethe-Bloch formula, it gives a value which is proportional to the atomic number of the incoming cosmic ray generating the event inside the detector. Almost all the peaks are clearly visible up to nickel ($Z = 28$), except those hidden by the tails of the highest adjacent peaks (P, Mn, Co).

Furthermore, the preliminary proton and helium fluxes have been analyzed by using the energy deposition measurement with the BGO calorimeter. Figure 8 shows the preliminary proton flux as a function of energy measured with DAMPE (see ref. [12]), compared with the results obtained by other experiments and it shows a good agreement with them. The same agreement can be seen in the helium flux in fig. 9 (see ref. [14]).

5. – Conclusions and outlooks

The first preliminary DAMPE results have been discussed here. By using the only PSD, we have a very good charge spectrum, clearly observing the peaks of almost all the nuclei from protons to nickel ($Z = 1$–28). Preliminary proton and helium fluxes, obtained with all the data collected by DAMPE, the wide accessible energy ranges (5 GeV–10 TeV for electrons and γ-rays and 50 GeV–100 TeV for protons and heavier nuclei) and the high energy resolution ($\sim 1.5\%$ for electrons/γs and $< 40\%$ for nuclei, both at 800 GeV), show a good agreement with already existing experiments.

The next goal for the DAMPE experiment consists in reaching the energy of 100 TeV for the measurement of proton and helium fluxes, respectively, in order to significantly improve our knowledge about the origin and the acceleration and propagation mechanisms of Cosmic Rays.

REFERENCES

[1] Aguilar M. *et al.*, *Phys. Rev. Lett.*, **110** (2015) 141102.
[2] Atwood B. *et al.*, *Astrophys. J.* **697** (2009) 1071.
[3] Menn W. *et al.*, *Adv. Space Res.*, **51** (2013) 209.
[4] DAMPE Collaboration, *Nature*, **552** (2017) 63.
[5] DAMPE Collaboration (Chang J. *et al.*), *Astropart. Phys.*, **95** (2017) 6.
[6] Birks J. B., *The Theory and Practice of Scintillation Counting: International Series of Monographs in Electronics and Instrumentation* (Elsevier) 2013.
[7] Zhang Y. *et al.* on behalf of the DAMPE Collaboration, *PoS*, **ICRC2017** (2017) 168.
[8] Aguilar M. *et al.*, *Phys. Rev. Lett.*, **114** (2015) 171103.
[9] Adriani O. *et al.*, *Science*, **332** (2011) 69.
[10] Panov A. D. *et al.*, *Bull. Russ. Acad. Sci. Phys.*, **73** (2009) 564.
[11] Yoon Y. S. *et al.*, *Astrophys. J.*, **839** (2017) 5.
[12] Yue C. *et al.* on behalf of the DAMPE Collaboration, *PoS*, **ICRC2017** (2017) 1076.
[13] Aguilar M. *et al.*, *Phys. Rev. Lett.*, **115** (2015) 211101.
[14] Gallo V. *et al.* on behalf of the DAMPE Collaboration, *PoS*, **ICRC2017** (2017) 169.